Evidence of Enhanced Hypersensitive Transition in Erbium-Doped Fibers With Different Al_2O_3 Content

Shunsuke Ono and Setsuhisa Tanabe

***Abstract*—Precise spectroscopic absorption measurements of erbium-doped aluminosilicate fibers with different Al_2O_3 content were performed with the Judd–Ofelt analysis. From the Judd–Ofelt analysis, the Ω_2 parameters of Er^{3+} ions in these fibers were found to be about three times as large as those in aluminosilicate bulk glasses. The enhancement of the Ω_2 parameters led to much stronger line strength of hypersensitive transitions in a fiber form than in a bulk glass form. This indicates that the distortion of the ligand field around the Er^{3+} ions are more enhanced in a fiber form than in a bulk glass form. Furthermore, the Ω_6 and the Ω_2 parameters increased with an increase of q content up to 20 000 ppm. This Al_2O_3-content dependence of the Ω_6 parameter was consistent with that of the line strength and the spontaneous emission probabilities of the transition corresponding to the $^4I_{13/2} \rightarrow {}^4 I_{15/2}$.**

***Index Terms*—Erbium, glass, optical amplifiers, optical materials, optical spectroscopy.**

I. Introduction

SILICA-BASED erbium-doped fiber amplifier (EDFA) has been a key device in the telecommunication system based on wavelength division multiplexing (WDM). This is because EDFA uses the emission transition corresponding to the $^4I_{13/2} \rightarrow {}^4 I_{15/2}$ of Er^{3+} ion and can amplify the light signal in the *C*-band wavelength region (1530–1570 nm), which is consistent with the low-loss wavelength region of telecom silica fibers.

On the other hand, there is urgent demand for optical amplifiers with a wide and flat gain spectrum due to the rapid increase of information traffic. Many studies about nonsilicate based optical amplifier for new bands (*S*-band:1450–1530 nm, *L*-band:1570–1630 nm) have been performed in order to expand transmission bandwidth [1], [2]. However, the silica-based erbium-doped fiber (EDF) is still a promising candidate, not only for the *C*-band amplifier, but also for the *S*-band and *L*-band ones because of its high reliability and favorable properties for the optical transmission system. Today, many efforts to modify the properties of silica-based EDF are being made for application to new band amplifiers [3], extracting more potential abilities of erbium-doped silica-based glasses for advanced EDF. So far, spectroscopy of erbium-doped bulk glasses has been well studied in order to improve the properties of EDF [4]. However, as far as we know, few spectroscopic studies have been carried out based on the Judd–Ofelt analysis for Er^{3+} ions in fiber forms. Therefore, this study focuses on the precise spectroscopy and the Judd–Ofelt analysis of aluminosilicate EDF with different Al_2O_3 content in order to investigate the ligand field structure around the Er^{3+} ions in fiber forms. The basic optical properties of EDF with different Al_2O_3 content were investigated mainly by optical absorption measurements and analyzed precisely by the Judd–Ofelt theory. The effect of the Al_2O_3 content on the change of the ligand field in aluminosilicate EDFs will be discussed based on the coordination number of Al^{3+} in aluminosilicate EDF.

Manuscript received May 29, 2004; revised August 9, 2004.

The authors are with the Graduate School of Human and Environmental Studies, Kyoto University, Kyoto 606-8501, Japan (e-mail: shunsuke@gls.mbox.media.kyoto-u.ac.jp; stanabe@gls.mbox.media.kyoto-u.ac.jp).

Digital Object Identifier 10.1109/JQE.2004.837665

II. Experimental

A. Absorption Measurements of EDF

Four EDF samples with different Al_2O_3 content were used for investigating the compositional dependence of optical properties of EDF. The concentrations of Er_2O_3 and Al_2O_3 of four EDF samples are shown in Table I. The solid-state and optical parameters for Al_2O_3-doped silica-based EDF samples were used in the calculations for the cross section analysis and Judd–Ofelt analysis. The absorption spectrum of an aluminosilicate bulk glass whose composition was the same as that of an aluminosilicate EDF sample (Al_2O_3 content: 20 000 ppm) was also examined. The refractive index of EDF samples at 1310 nm was measured using a reflectometer, (Ando, AQ7413). Absorption spectra of EDF in the 1.5-μm region were measured with three tunable laser sources (Santec, TSL210) in the range of 1420–1640 nm and an optical spectrum analyzer (OSA) (Anritsu, MS9780A). The signal input power was -30 dBm in order not to saturate fiber loss. In the 1.5-μm region absorption measurement, fiber lengths of four EDFs were 1 m. The TSL and OSA were controlled by a personal computer using general purpose interface bus (GPIB). Loss was determined by detecting the peak power of a signal output power and subtracting a signal output power from a signal input power.

In order to carry out the Judd–Ofelt analysis, absorption measurements in the wavelength region from 400 to 1650 nm were also performed using a white light source (Ando, AQ4303B), a fiber-optic spectrometer (Ocean optics, USB2000), and the OSA.

B. Emission Measurements and Cross Section Analysis Based on McCumber Theory

Spontaneous emission of an EDF sample (Al_2O_3:20 000 ppm) was measured as side fluorescence at room temperature with a monochromator (Nikon G250) and a photodetector (Electro Optical Systems). Each EDF was pumped by a 980-nm laser diode (LD). The pump power was 150 mW, which was

TABLE I
BASIC SOLID-STATE PARAMETERS FOR EDF SAMPLES

sample	Er_2O_3 (ppm)	Al_2O_3 (ppm)	ρ_{Er2O3} ($/\times 10^{18} cm^3$)	$n_{1.3\,\mu m}$ (-)	λ_{mean}(nm) (1.5 μ m region)
EDF1	780	5000	5.21	1.476	1523.8
EDF2	880	10000	5.53	1.475	1525.3
EDF3	630	20000	4.10	1.474	1524.6
EDF4	800	40000	5.44	1.481	1523.9

enough power to achieve the population inversion. An experimental emission cross section was calculated using the obtained emission spectrum. In addition, a theoretical emission cross section of the EDF sample (Al_2O_3:20 000 ppm) was also calculated using the measured absorption cross section σ_a through the McCumber relation [5] as follows:

$$\sigma_e(\nu) = \sigma_a \exp\left[\frac{(E_0 - h\nu)}{\kappa T}\right] \cdot \frac{1 + \sum_{j=2}^{8} 7\exp\left(-\frac{\Delta E_{1j}}{kT}\right)}{1 + \sum_{j-2}^{7} 6\exp\left(-\frac{\Delta E_{2j}}{kT}\right)} \quad (1)$$

where E_0 is the separation energy between the lowest component of each manifold and assumed to be 6535 cm^{-1} ($\lambda = 1530$ nm). ΔE_{1j} and ΔE_{2j} are the differences in energy between the jth and the lowest component of the $^4I_{13/2}$ and the $^4I_{15/2}$ level. Here, we supposed that the adjacent components in the same manifold are separated by the same energy δE_1 and δE_2. Comparison of the experimental cross section with the theoretical one was performed in the next section.

III. RESULTS AND DISCUSSION

A. Al_2O_3 Dependence of Absorption Cross Section

Fig. 1(a) shows the absorption cross section σ_a calculated from the loss spectra. σ_a showed the Al_2O_3 dependence and increased about double with the increasing content of Al_2O_3 up to 20 000 ppm. Fig. 1(b) shows the comparison of the experimental emission cross section for Al_2O_3-doped EDF (Al_2O_3:20 000 ppm) with theoretical one. The theoretical emission cross section was calculated from the absorption cross section using McCumber relation mentioned above. The shape of the theoretical cross section shows good agreement with that of experimental one.

Fig. 2 shows the line strength $S_{JJ'}$ corresponding to the 1.5-μm transition and the spontaneous probability $A_{JJ'}$ of the $^4I_{13/2}$ $-^4$ $I_{15/2}$ transition and the measur-ed lifetime of the $^4I_{13/2}$, τ_f.

According to the Judd–Ofelt theory, the line strength $S_{JJ'}$ is related to the integrated absorption cross section of the 1.5-μm transition in Fig. 1(b) as follows:

$$S_{JJ'} = \frac{3hc(2J+1)}{8\pi^3 e^2 \lambda_{\text{mean}} \rho} n \left[\frac{9}{(n^2+2)^2}\right] \int_{\text{band}} k(\lambda) d\lambda \quad (2)$$

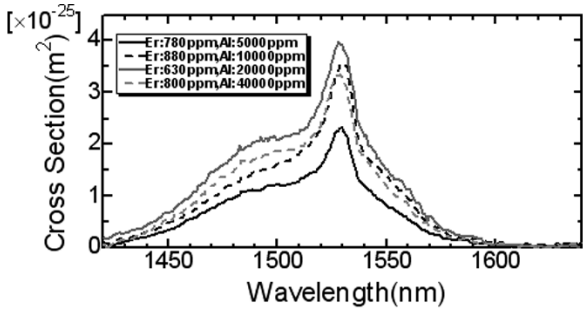

(a)

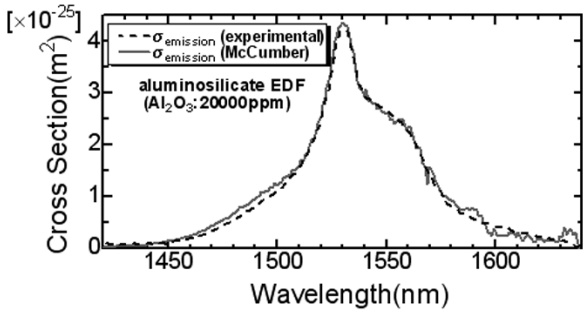

(b)

Fig. 1.(a) Absorption cross-section spectra for Al_2O_3-doped EDF in a 1.5-μm region. (b) Comparison of the experimental emission spectra for Al_2O_3-doped EDF (Al_2O_3:20 000 ppm) with the theoretical one based on McCumber theory.

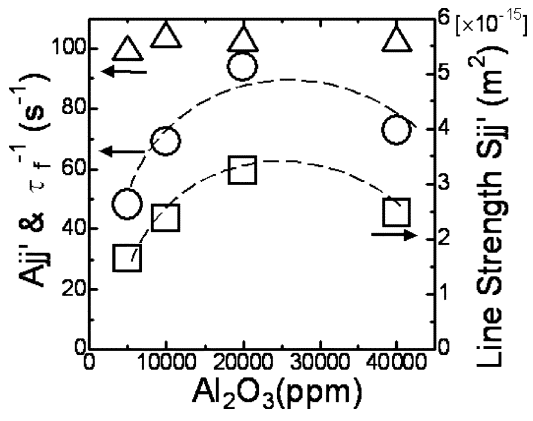

Fig. 2. Al_2O_3 dependence of $S_{JJ'}$ (open square), $A_{JJ'}$ (open circle), and τ_f (open triangle).

where $k(\lambda)$ is the absorption coefficient at λ, λ_{mean} is the mean wavelength of the absorption band, ρ is the concentration of Er^{3+} ions per unit volume, h is Planck's constant, c is the

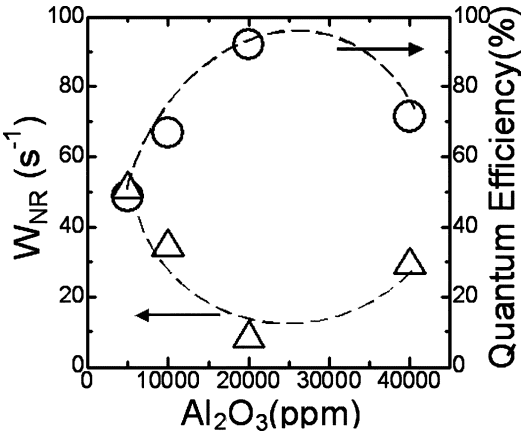

Fig. 3. Al_2O_3 dependence of $W_{\rm NR}$ and QE.

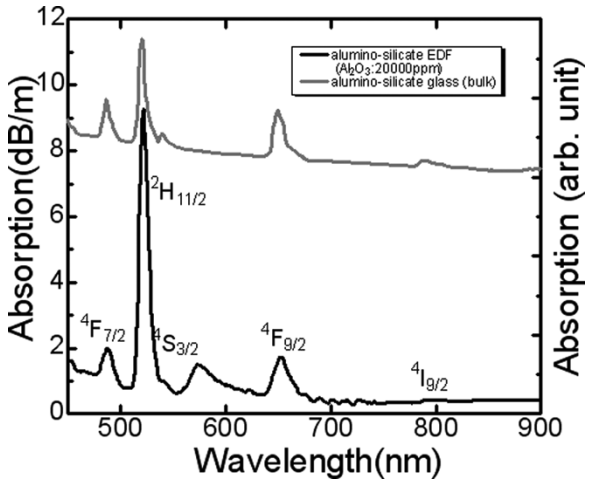

Fig. 4. Comparison of absorption spectra for Al_2O_3-doped EDF with an aluminosilicate bulk glass.

speed of light, e is the elementary charge, and n is the refractive index. The refractive indexes of the core of the EDF were about 1.47 and showed little Al_2O_3-content dependence as shown in Table I. J is the total angular moment of the initial state, which is the $^4I_{15/2}$, and J' is that of the final state $^4I_{13/2}$ for the 1.5 μm transition. The spontaneous emission probability $A_{JJ'}$ is proportional to the line strength $S_{JJ'}$ using local field correction factor $(n^2+2)^2/9$ through the relation

$$A_{JJ'} = \frac{64\pi^2 e^2}{3h(2J+1)\lambda^3_{\rm mean}} n \left[\frac{(n^2+2)^2}{9}\right] S_{JJ'}. \quad (3)$$

As shown in Fig. 2, both the $S_{JJ'}$ and $A_{JJ'}$ increased with the increase of Al_2O_3 content up to 20 000 ppm and decreased over 20 000 ppm of Al_2O_3. The increase of $S_{JJ'}$ and $A_{JJ'}$ is considered to be caused by the increase of the electric-dipole component of $S_{JJ'}$ because the magnetic-dipole component of $S_{JJ'}$ is independent of the change of ligand field. On the other hand, τ_f showed little Al_2O_3 dependence and was about 10 ms, which is a typical value for the lifetime of the $4I_{13/2}$ level of Er^{3+}. Fig. 3 shows the nonradiative decay rate $W_{\rm NR}$ and quantum efficiency (QE). Using τ_f and $A_{JJ'}$, $W_{\rm NR}$ and QE are expressed as

$$W_{\rm NR} = \tau_f^{-1} - \sum_{J'} A_{JJ'} \quad (4)$$

$$\mathrm{QE} = \frac{\sum_{J'} A_{JJ'}}{W_{NR} + \sum_{J'} A_{JJ'}}. \quad (5)$$

B. Al_2O_3 Dependence of Ω_6 Parameters in Fibers

In order to investigate the Al_2O_3-content dependence of the Ω_t (t =2,4,6) parameters of doped Er^{3+} ions, we analyzed each absorption band that corresponded to the optical transition between 4f-multiplets of Er^{3+} ions using the Judd–Ofelt theory.

Fig. 4 shows the comparison of the absorption spectrum of EDF (Al_2O_3 content: 20 000 ppm) with that of an aluminosilicate bulk glass whose composition was the same as that of an aluminosilicate EDF sample (Al_2O_3 content: 20 000 ppm).

We can see the four absorption bands corresponding to the transitions from the $^4I_{15/2}$ to the $^4F_{9/2}$, $^4S_{3/2}$, $^2H_{11/2}$, and $^4F_{7/2}$. The absorption spectrum of the $^2H_{11/2}$ is remarkably larger in aluminosilicate EDF than of those in aluminosilicate bulk glass. This enhancement of the absorption peak of the $^2H_{11/2}$ was also observed in other erbium-doped fibers.

Fig. 5 shows the Al_2O_3-content dependence of the Judd–Ofelt intensity parameters Ω_2, Ω_4, and Ω_6 calculated from the line strength absorption spectra in 400–1650 nm. The measured line strength could be matched with the best fit Ω_t results to 10%–15% (rms) accuracy for all the aluminosilicate EDFs examined. As shown in Fig. 5, the Ω_6 parameter was found to increase with the increase of the Al_2O_3 content up to 20 000 ppm. On the other hand, according to the Judd–Ofelt theory, $S_{JJ'}$ was defined with the Ω_t parameter as follows:

$$S^{\rm ed}[S,L,J;S',L',J'] = \sum_{t=2,4,6} \Omega_t \times \left|\left\langle 4f^N S,L,J \left| U^{(t)} \right| 4f^N S',L',J' \right\rangle\right| \quad (6)$$

where $\langle 4f^N S,L,J|U^{(t)}|4f^N S',L',J'\rangle$ denotes the reduced matrix element. The coefficients Ω_2, Ω_4, and Ω_6 contain the effects of odd-symmetry crystal-field terms. In particular, the $S_{JJ'}$ of the electric dipole components of the 1.5-μm transition with Al_2O_3 content is given by [6]

$$S^{\rm ed}\left[^4I_{\frac{13}{2}};^4I_{\frac{15}{2}}\right] = 0.019\,\Omega_2 + 0.118\,\Omega_4 + 1.462\,\Omega_6. \quad (7)$$

While $S_{\rm ed}$ is a function of glass structure and composition using the Ω_t ($t=2,4,6$) parameter, $S_{\rm md}$ is independent of the ligand fields and is characteristic to the transition determined by the quantum numbers. For the transition between the states which meet the transition selective rules $\Delta S = \Delta L = 0$, $\Delta J = 0$, and ± 1, there exists the contribution of magnetic dipole transition [7], [8]. Therefore, the increase of total line strength $S_{JJ'}$ of the 1.5-μm transition with the increase of Al_2O_3 shown in Fig. 2 can be largely dominated and explained well by the increase of the Ω_6 intensity parameter shown in Fig. 5.

The value of the Ω_6 particularly tends to be affected by the basicity of glass and is known empirically to become larger as the basicity decreases [9]. Therefore, the increase of the Ω_6 parameter indicates that the increase of Al_2O_3 weaken covalent

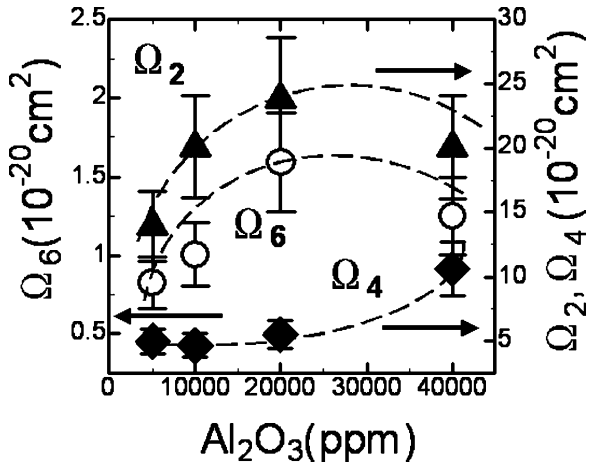

Fig. 5. Al_2O_3-content dependences of the Judd–Ofelt intensity parameter Ω_2, Ω_4, and Ω_6.

character of Er–O as a results the formation of Si–O–Al. Generally, it is known that the coordination number of Al^{3+} becomes smaller in the host glasses with higher basicity and the production of four-coordinated Al^{3+} is enhanced compared to the formation of six-coordinated Al^{3+} [10]. Moreover, the optical basicity of four-coordinated Al^{3+} in the network of SiO_4 is known to be smaller than that of six-coordinated Al^{3+} (microscopic λ of Si-O-Al is 0.59 for four-coordinated Al^{3+} and 0.65 for six-coordinated Al^{3+}) [11]. Therefore, Er^{3+} ions have the possibility to be surrounded by more four-coordinated Al^{3+} ions rather than six-coordinated Al^{3+} ions with an increase of Al_2O_3. The decrease of the basicity around Er^{3+} sites up to 20 000 ppm of Al_2O_3 content can be considered in particular as the result of the increase in the number of the four-coordinated Al^{3+} surrounds the Er^{3+} site.

C. Al_2O_3 Dependence of Ω_2 Parameters in Fibers

As shown in Fig. 5, the value of the Ω_2 parameter in fibers takes about three times as large a value as those in aluminosilicate and borate bulk glasses [12] ($\Omega_{2:(\mathrm{Al-Si})\mathrm{glass}} = 4.6$, $\Omega_{2:(\mathrm{Bo})\mathrm{glass}} = 3.21$), which corresponds to the experimental results of a strong absorption band of the $^2H_{11/2}$ as shown in Fig. 4. The relation between the Ω_t (t =2, 4, 6) paramete, r and the electric-dipole line strength component of $^2H_{11/2}$ is given by

$$S^{\mathrm{ed}}\left[{}^2H_{\frac{11}{2}};{}^4I_{\frac{15}{2}}\right] = 0.7056\,\Omega_2 + 0.4109\,\Omega_4 + 0.0870\,\Omega_6. \quad (8)$$

This relation shows that the electric-dipole line strength of the $^2H_{11/2} - {}^4I_{15/2}$ is largely dominated by the value of the Ω_2 parameter. Therefore, the experimental results of a strong absorption band of the $^2H_{11/2}$ can be explained well by (11). In case of Er^{3+}, the electric-dipole line strength of the $^4G_{11/2} - {}^4I_{15/2}$ is also expected to show very strong absorption in fibers because the reduced matrix element $\langle\|U^{(2)}\|\rangle$ of the $^4G_{11/2} - {}^4I_{15/2}$ takes dominantly large value similar to that of the $^2H_{11/2} - {}^4I_{15/2}$

$$S^{\mathrm{ed}}\left[{}^4G_{\frac{11}{2}};{}^4I_{\frac{15}{2}}\right] = 0.9178\,\Omega_2 + 0.5271\,\Omega_4 + 0.1197\,\Omega_6. \quad (9)$$

Both the $^4G_{11/2} - {}^4I_{15/2}$ and the $^2H_{11/2} - {}^4I_{15/2}$ are called the hypersensitive transition that is dominated and enhanced by the large Ω_2 parameter. It is known that the value of the Ω_2 is raised drastically by lowering the symmetry of the rare-earth ligand field [13]. According to the Judd–Ofelt theory, the Ω_2 critically dominates the hypersensitive transition that was reported to be largely affected by the polarized distortion of the ligand field [14], [15]. Therefore, the Er^{3+} sites in fibers are considered to have larger polarization or asymmetric distortion than in bulk glasses. Moreover, the Ω_2 also increased with the increase of the Al_2O_3 content. Considering the Al_2O_3 dependence of the Ω_6 parameter, this indicates that the substitution of six-coordinated Al^{3+} for four-coordinated Al^{3+} with the increase of Al_2O_3 may occur. Therefore, high Al_2O_3 doping is likely to enhance the distortion of the ligand field of Er^{3+} site caused by the existence of four- and six-coordinated Al^{3+}.

IV. Conclusion

The $S_{JJ'}$ and the $A_{JJ'}$ of the Er:1.5-μm transition increased with the increase of Al_2O_3 content in EDF. The Ω_6 parameter increased with the increase of Al_2O_3 content, which can be explained by the compositional dependence of the $S_{JJ'}$ of the Er:1.5-μm transition . These results indicate that a decrease of local basicity occurs by adding Al_2O_3. The Ω_2 parameter in a fiber form was found to be about three times as large as those in a bulk glass form and also increased with an increase of Al_2O_3 content. The decrease of the local basicity and the symmetry of the Er^{3+} ligand field in aluminosilicate EDF samples are attributed to the increase of four-coordinated Al^{3+}.

References

[1] Y. Ohishi, A. Mori, M. Yamada, H. Ono, Y. Nishida, and K. Oikawa, "Gain characteristics of tellurite-based erbium-doped fiber amplifiersfor 1.5-mm broadband amplification," *Opt. Lett.*, vol. 23, pp. 274–276, 1998.

[2] S. Aozana, T. Kanamori, K. Hoshino, and M. Shimizu, "Gain-shifted thulium-doped fiber amplifiers employing novel high concentration doping technique," *Electron. Lett.*, vol. 36, pp. 418–419, 2000.

[3] E. Ishikawa, M. Nishihara, Y. Sato, C. Ohshima, Y. Sugaya, and J. Kumasako, "Novel 1500 nm-band EDFA with discrete Raman amplifier," in *Proc. ECOC*, 2001, paper PD.A.1.2.

[4] E. Snoeks, P. G. Kik, and A. Polman, "Concentration quenching in erbium implanted alkali silicate glasses," *Opt. Mater.*, vol. 5, pp. 159–167, 1996.

[5] D. E. McCumber, "Theory of phononterminated optical masers," *Phys. Rev. A, Gen. Phys.*, vol. 134, pp. A299–A306, 1964.

[6] M. J. Weber, "Probabilities for radiative and nonradiative decay of Er^{3+} in LaF_3," *Phys. Rev. A, Gen Phys.*, vol. 157, pp. 262–272, 1967.

[7] B. R. Judd, "Optical absorption intensities in rare-earth ions," *Phys. Rev. A, Gen Phys.*, vol. 127, pp. 750–761, 1962.

[8] G. S. Ofelt, "Intensities of crystal spectra of rare-earth ions," *J. Chem. Phys.*, vol. 37, pp. 511–520, 1962.

[9] S. Tanabe and T. Hanada, "Local structure and 1.5 μm quantum efficiency of erbium doped glasses for optical amplifiers," *J. Non-Cryst. Solids*, vol. 196, pp. 101–105, 1996.

[10] H. Kawazoe, "Coordination number and chemical shift in $K\alpha_{12}$ emission of Mg^{2+} in oxide glasses," *J. Non-Cryst. Solids*, vol. 42, pp. 281–285, 1980.

[11] J. A. Duffy and M. D. Ingram, "An interpretation of glass chemistry in terms of the optical basicity concept," *J. Non-Cryst. Solids*, vol. 21, pp. 373–410, 1976.

[12] S. Tanabe, T. Ohyagi, S. Todoroki, T. Hanada, and N. Soga, "Relation between the Ω_6 intensity parameter of Er^{3+} ions and the ^{151}Eu isomer shift in oxide glasses," *J. Appl. Phys.*, vol. 73, pp. 8451–8454, 1993.

[13] C. K. Jørgensen and B. R. Judd, "Hypersensitive pseudoquadrupole transitions in lanthanides," *Mol. Phys.*, vol. 8, pp. 281–290, 1964.

[14] M. Eyal, R. Reisfeld, A. Schiller, C. Jacobini, and C. K. Jørgensen, "Energy transfer between manganese(II) and thulium(III) in transition-metal fluoride glasses," *Chem. Phys. Lett.*, vol. 140, pp. 595–602, 1987.

[15] R. D. Peacock, "The intensities of lanthanide f-f transitions," in *Structure and Bonding*. Berlin, Germany: Springer-Verlag, 1975, vol. 22, pp. 83–121.

Shunsuke Ono received the B.Sc. and M.Sc. degrees in physics from Kobe University, Kobe, Japan in 1997 and 1999, respectively. He is currently working toward the Ph.D. degree at Kyoto University, Kyoto, Japan.

In 1999, he joined Nihon Electronic Company (NEC), Kawasaki, Japan, where he was engaged in the research and development of the 10-Gb/s transpacific optical submarine transmission system using the dense wavelength-division-multiplexing technique (DWDM). His present research interests are centered around the characterization of optical properties of optical amplifiers for transmission systems, which includes the physical dynamics of the gain spectral-hole burning (GSHB) in aluminosilicate erbium-doped fibers.

Setsuhisa Tanabe received the B.S., M.S., and the Ph.D. degrees from Kyoto University, Kyoto, Japan, in 1986, 1988, and 1993, respectively, all in industrial chemistry.

In 1990, he became an Assistant Professor with the Faculty of Integrated Studies, Kyoto University. From 1996 to 1997, he was a Visiting Scientist with the Department of Ceramic Science and Engineering, Rutgers University, New Brunswick, NJ. In 2001, he became an Associate Professor with the Graduate School of Human and Environmental Studies, Kyoto University. His current research interests include optical functions, structural analysis and characterization of solids, and the relationship between structure and optical properties of rare-earth-doped materials.